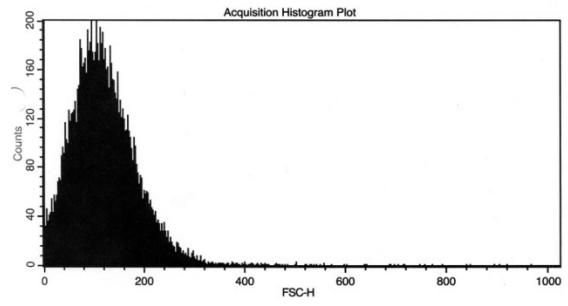
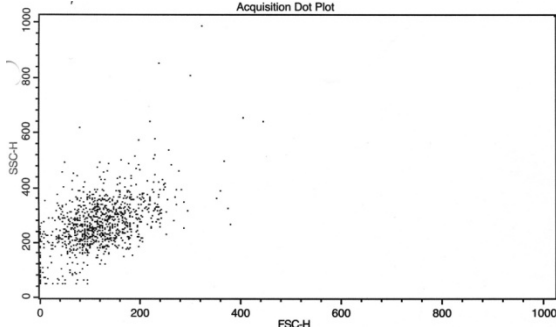
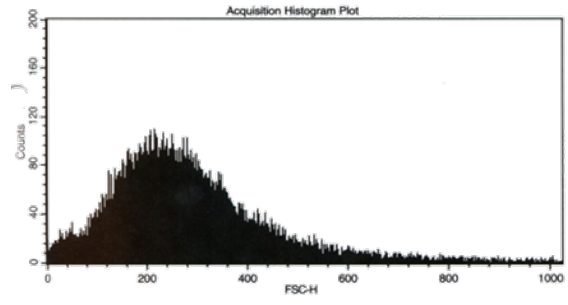
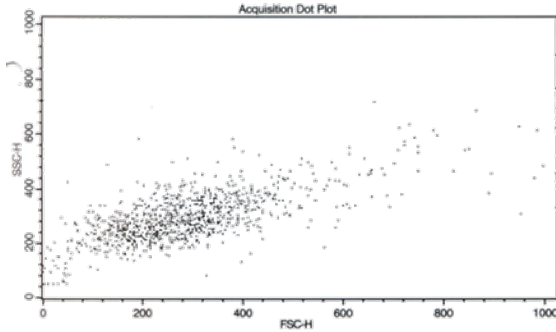


A.

CS109

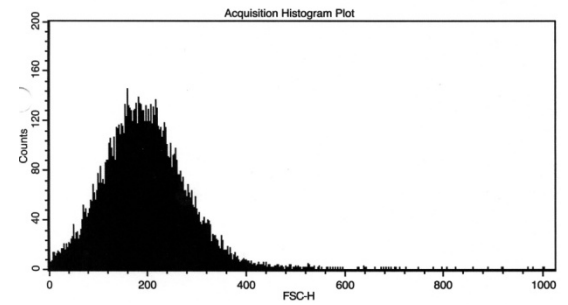
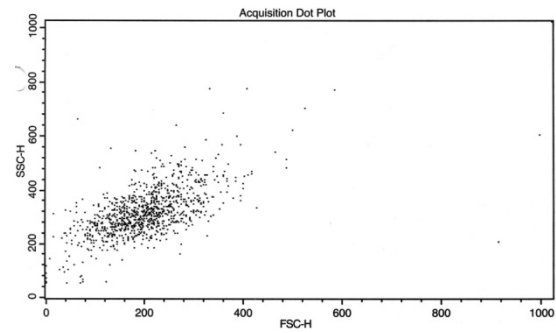


CS315

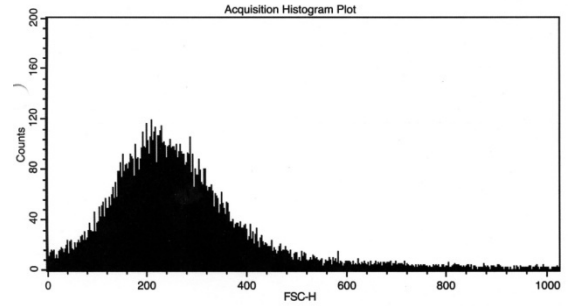
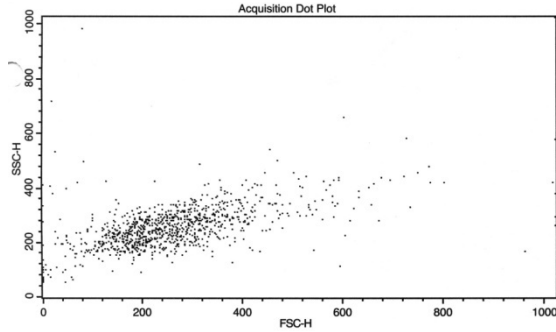


B.

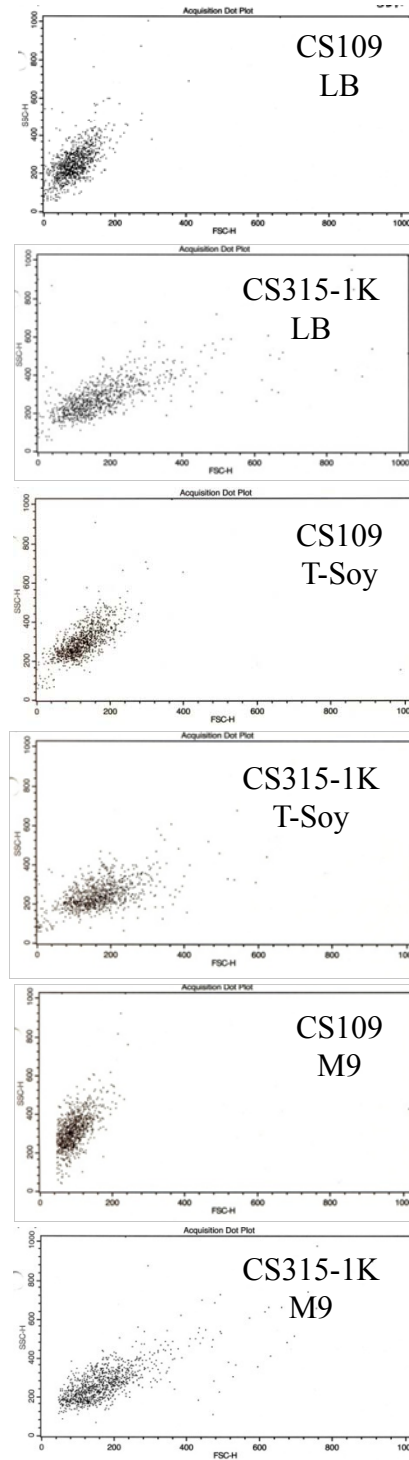
CS109



CS315

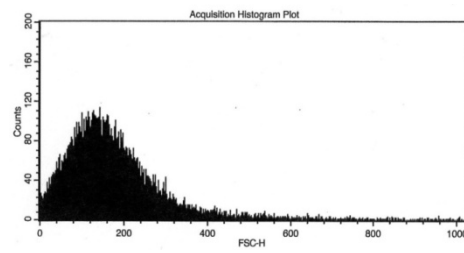
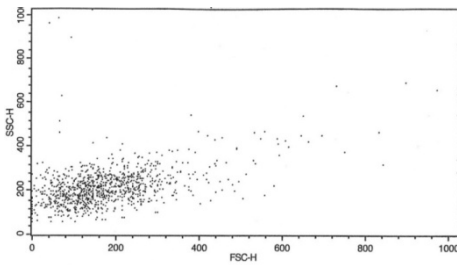


Supplemental Figure S1. FACS analyses of cells harvested at different optical densities. CS109 and CS315-1K cultures harvested at: A) an OD₆₀₀ of ~0.40, or B) an OD₆₀₀ of ~0.50. Differences between the strains are easier to see when harvested when the OD₆₀₀ = 0.40.

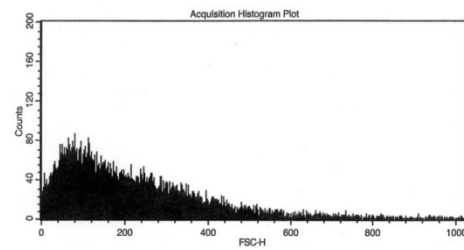
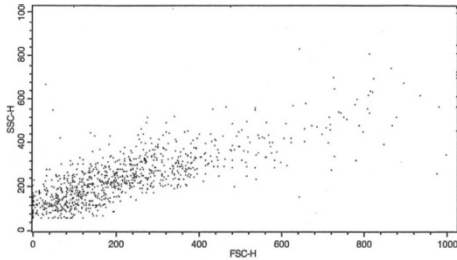


Supplemental Figure S2. FACS dot plots of CS109 and CS315-1K grown in three types of media. Cultures grown in LB were more readily differentiated from one another than cultures grown in T-soy or M9-minimal broths.

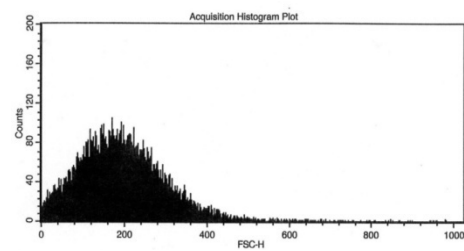
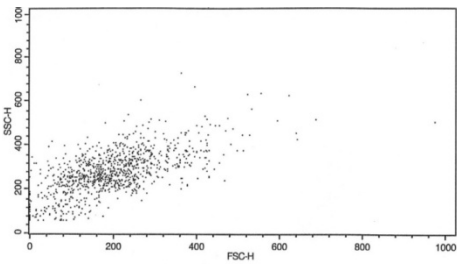
CS315-1K



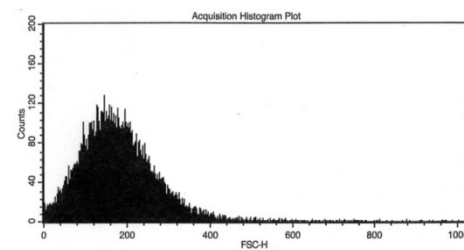
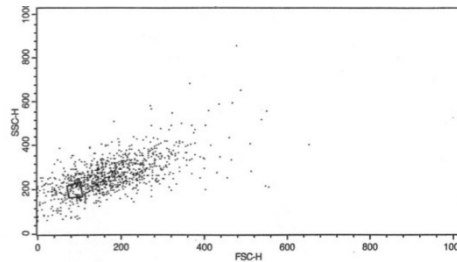
-1F



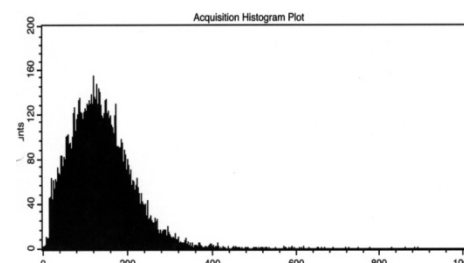
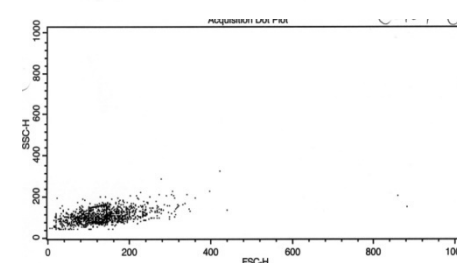
-4F



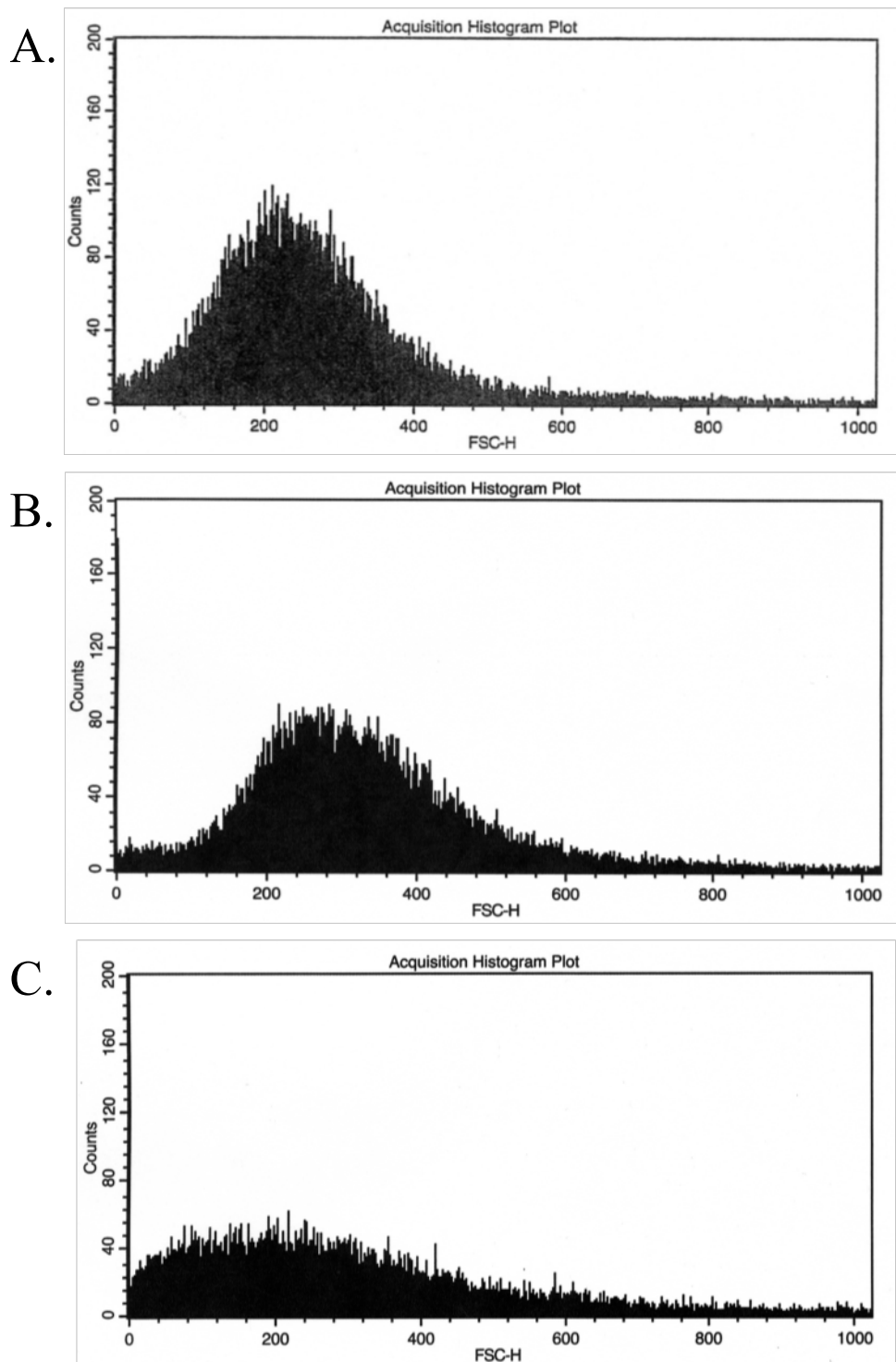
-5F



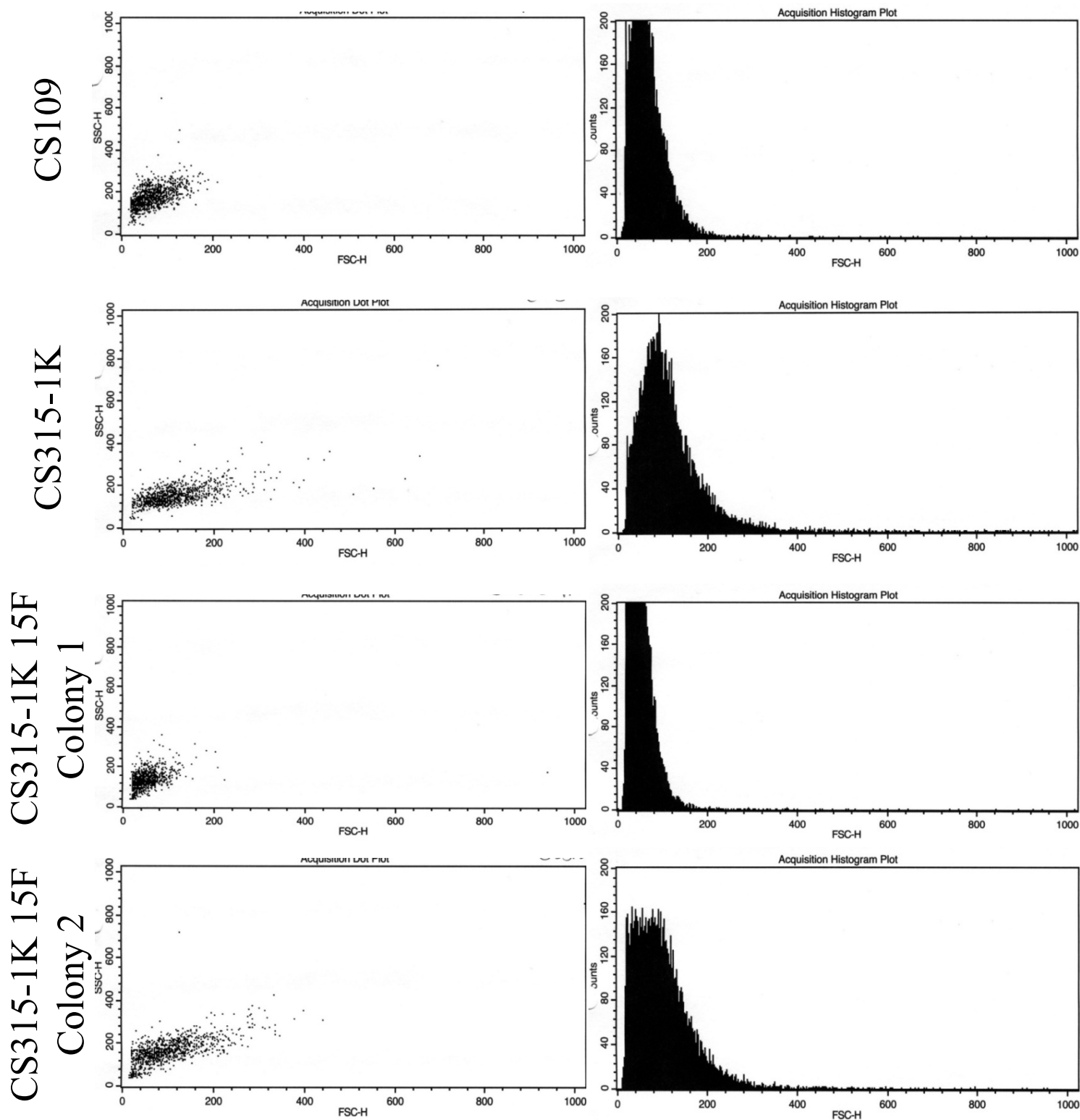
-15F



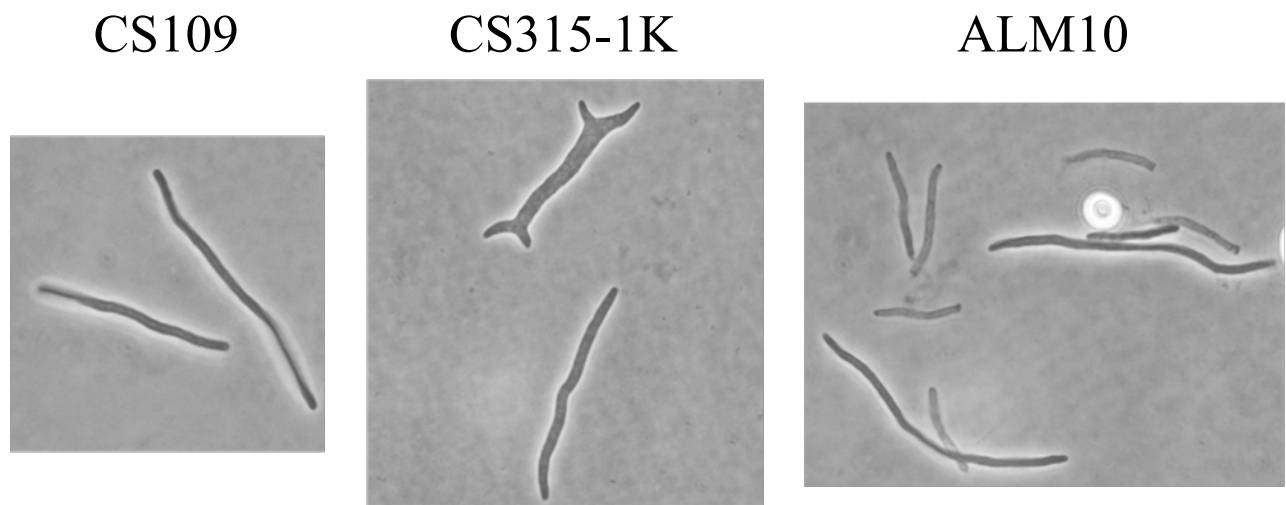
Supplemental Figure S3. Population distributions of CS315-1K cells collected different iterations of FACS sorting (denoted as “#F”). After one round of sorting and regrowth, the distribution of the population (C315-1K-1F) was shifted much further to the right, indicating that the cells were more abnormally shaped than were those of its parent, CS315-1K. CS315-1K-4F and CS315-1K-5F represent enriched populations after four and five rounds of sorting, respectively. The CS315-1K-5F population distribution (both dot plot and histogram) has moved further to the left, becoming more like the wild type distribution of CS109. At this point the plot and histogram of the sorted cells fall to the left of the original CS315-1K mutant strain (i.e., the cell shapes have become more normal). The bottom graphs show the shape distribution of CS315-1K-15F (the population after 15 rounds of sorting) from which *E. coli* ALM10 was isolated. The distribution of CS315-1K-15F (both dot plot and histogram) is more like that of CS109 and is far removed from the distribution of CS315-1K.



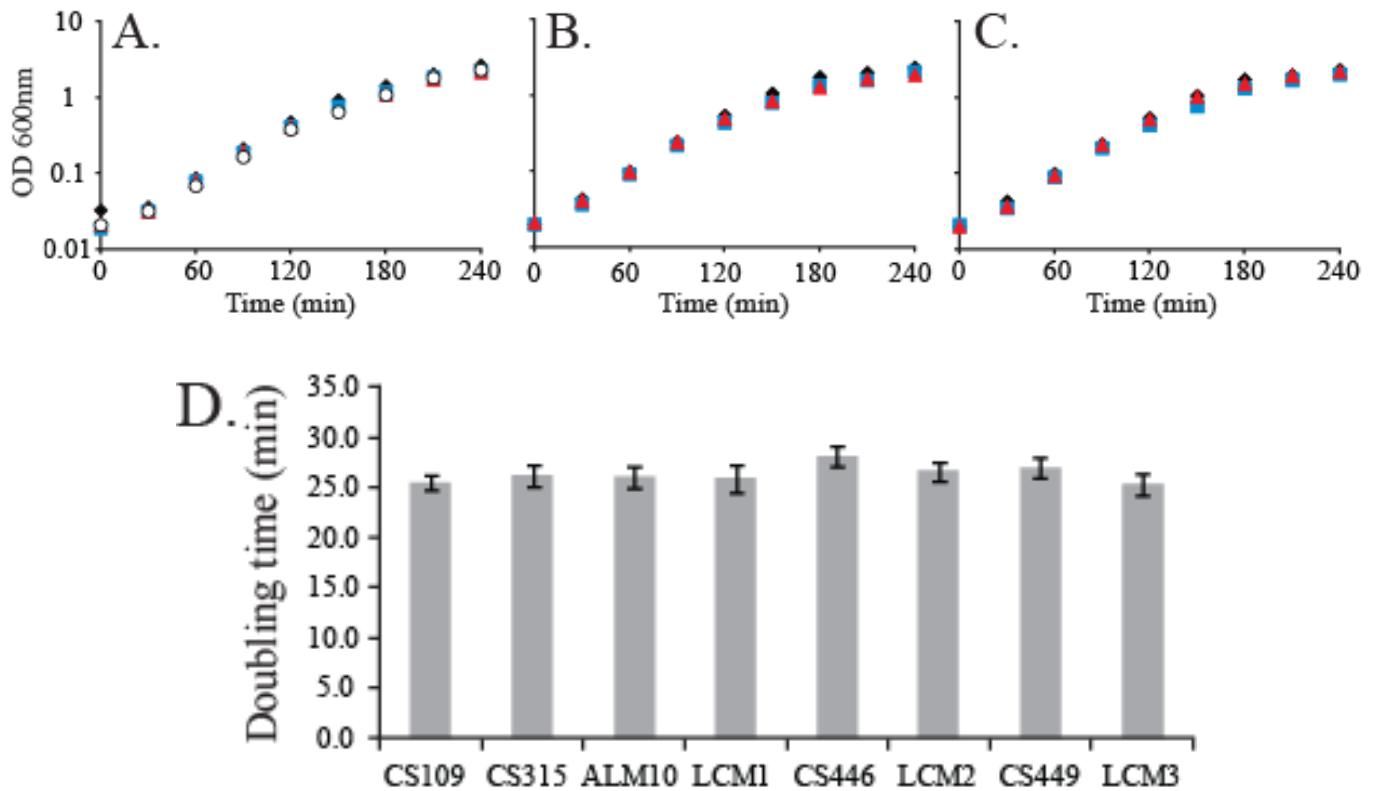
Supplemental Figure S4. Shape distribution of a control culture of CS315-1K subjected to daily cycles of regrowth but without FACS sorting. Over time, the shape distributions of CS315-1K cells in continuous culture became more aberrant rather than becoming more normal, as was observed during FACS enrichment. A. CS315-1K cells before regrowth or sorting. B. CS315-1K cells after one cycle of growth (one day) plus regrowth. C. CS315-1K cells after six cycles of growth (6 days).



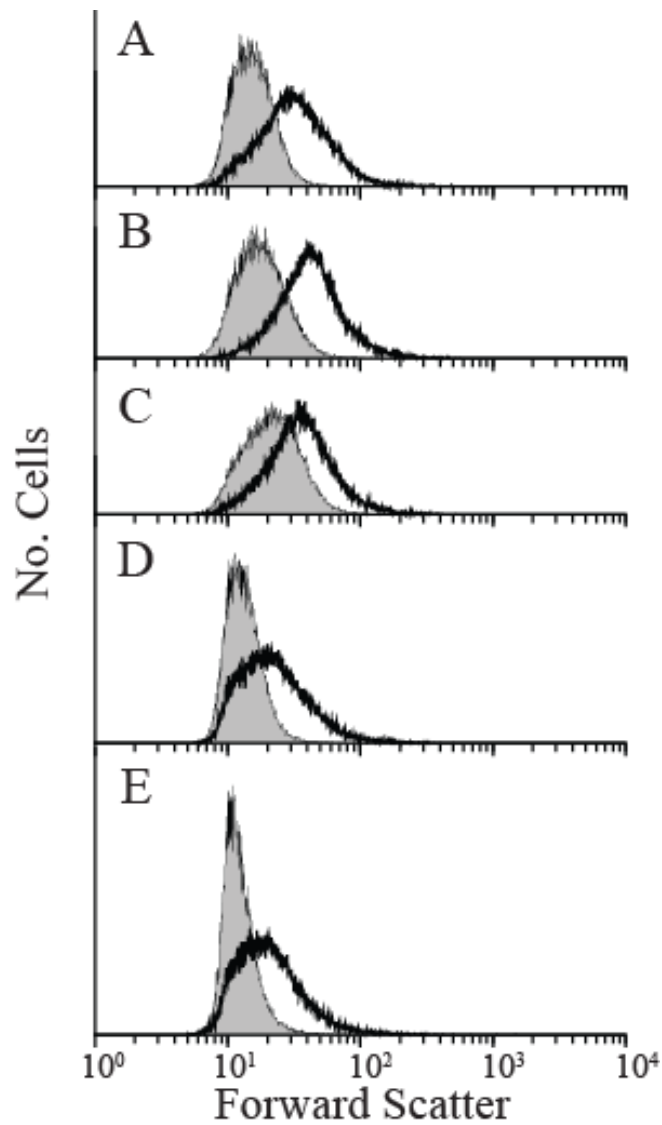
Supplemental Figure S5. FACS analysis of two single colonies isolated from the mass culture of CS315-1K-15F. The shape distribution of cells from “Colony 1” is similar to that of CS109 and most likely contains one or more suppressor mutations. The shape distribution of cells from “Colony 2” is similar to that of CS315-1K and probably does not contain suppressor mutations. “Colony 1” was renamed ALM10 and was studied further.



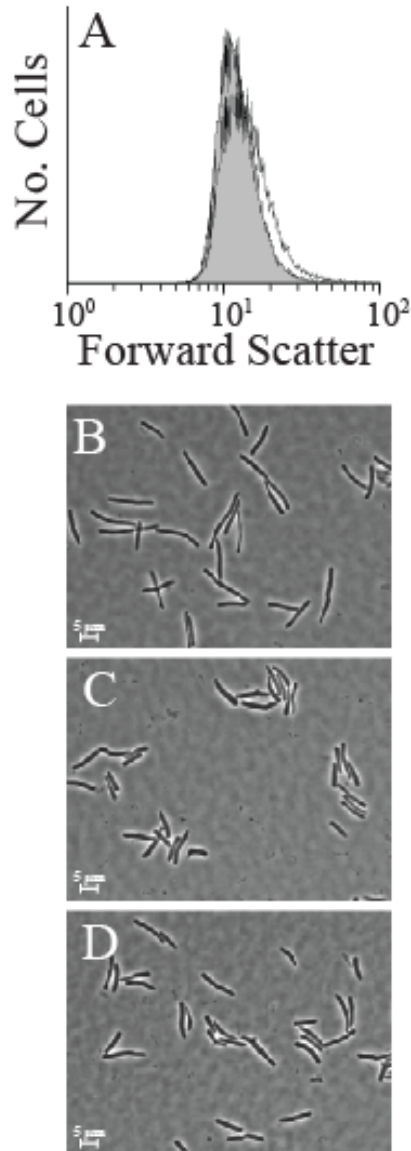
Supplemental Figure S6. Microscopic morphologies of CS109, CS315-1K and ALM10. Cells were grown in the presence of aztreonam (5 $\mu\text{g/ml}$) to amplify slight shape defects. ALM10 cells treated in this way formed straight filaments of uniform diameter, like those of the wild type strain CS109, instead of cells with irregular diameters and branches, like those of its parent, CS315-1K.



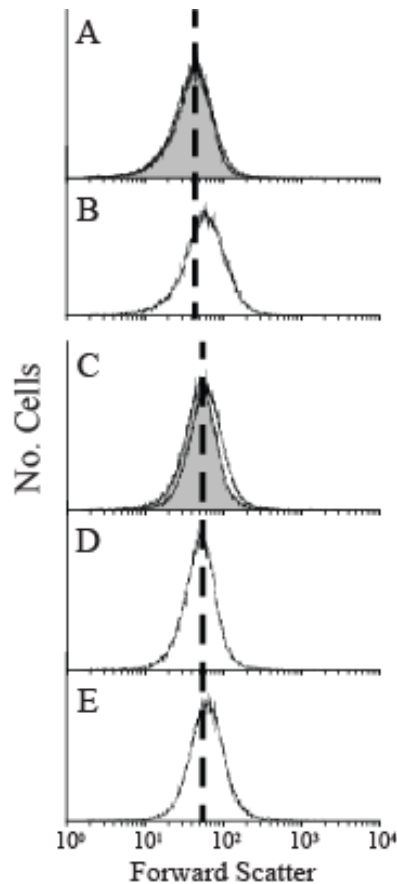
Supplemental Figure S7. Suppressors of cell shape do not affect growth rates in LB. A. CS109 (black diamonds), CS315 (blue squares), ALM10 (red triangles), and LCM1 (white circles). B. CS109 (black diamonds), CS446 (blue squares), and LCM2 (red triangles). C. CS109 (black diamonds), CS449 (blue squares), and LCM3 (red triangles). The growth curves are representative of independent experiments. D. Doubling times of strains in exponential growth phase. Values are the average of three experiments, with standard deviations as indicated.



Supplemental Figure S8. CS315-1K cells retain a poor cell shape distribution when the population is subjected to sequential growth iterations without sorting. Grey-filled peaks, the parental CS109 shape distributions. Black graphed lines, the shape distributions of *E. coli* CS315-1K at: A) the start of the experiment, and after B) 1, C) 2, D) 3, and E) 4 growth passages without sorting.



Supplemental Figure S9. Potential shape suppressor mutants derived from *E. coli* CS456-1K. Every individual isolate that was tested retained an aberrant cell shape despite the fact that the enriched population as a whole displayed a relatively normal shape distribution. However, even though each isolate exhibited a shape distribution similar to that of the wild type CS109 strain, microscopic observations revealed that shape abnormalities were still present in high numbers. A. Shape distribution of a representative suppressor candidate. Grey peak, shape distribution of *E. coli* CS109. Black line, shape distribution of the potential suppressor mutant #43. B-D. Phase microscopy of CS109 (B), CS456-1K (C), and suppressor candidate #43 (D).



Supplemental Figure S10. Removal of AmpH but not PBP1A alters cell shape. A and B. Light scatter profiles of *E. coli* ALM10 (grey-filled peak) and its peak distribution (black dashed line). A. LCM9 (ALM10 Δ PBP1A), black curve. B. LCM5 (ALM10 Δ ampH), black curve. C-E. Light scatter profile of ALM10 containing the empty vector pLP8 (grey-filled peak) and its peak distribution (black dashed line). C. LCM5 containing the vector pLP8, black curve. D. LCM5 containing pLCM1 (expressing wild type AmpH), black curve. E. LCM5 pMEL1 (expressing active site mutant AmpHS87A), black curve.